International Journal of Solids and Structures 279 (2023) 112347

Contents lists available at ScienceDirect

International Journal of Solids and Structures

journal homepage: www.elsevier.com/locate/ijsolstr

The shear contribution to the equation of state: A universal law for the elastic moduli of solids

S.J. Burns [a,*], Sean P. Burns [b]

[a] Materials Science Program, Department of Mechanical Engineering, University of Rochester, Rochester, NY 14627-0132, USA
[b] Mesoscale and Microscale Meteorology Laboratory, National Center for Atmospheric Research, 3090 Center Green Drive, Boulder, CO 80301, USA

ARTICLE INFO

Keywords:
Thermoelasticity
Thermodynamics
Elastic properties of materials
Material science
Elastic moduli
Elasticity
Geophysics
Seismology
Solids equations of state

ABSTRACT

Cauchy's stress tensor, in the most generalized form, is known to be in two parts: a pressure plus octahedral shear stresses. Shear stress thermodynamics in pressurized and sheared systems are used to describe the physical shear properties of materials. Pressure alone does not fully describe solids although pressure is the basis for most equations of state. The thermal expansion coefficients are the major differences between normal and shear thermal strains. Shear-strain thermal expansion coefficients are central to predicting a material's shear properties. Shear thermodynamics through the entropy-stress components predicts shear moduli proportional to a power-law in the specific volume. The concept is applied to all elastic moduli in solids and structures. Extensive empirical evidence supports elastic moduli that depend only on specific volume. The evidence is very extensive and leads to a new, generalized, universal, elastic moduli concept; it applies to materials that support shear stresses i.e., solids. A shear equation of state is explored in detail with use of empirical data. The elastic moduli are proportional to a specific volume power-law; the volume is both pressure and temperature dependent.

1. Introduction

The thermal and elastic properties of solids have been of interest for a very long time. Physical and mechanical properties play a fundamental role in advancing technology and understanding complex phenomena. Physical properties at high temperatures and extreme pressures as in compressed materials are considered central for successful laser fusion energy production (Hicks et al., 2009; Craxton et al., 2015; Hu et al., 2010). A new high-pressure physics (Degtyareva, 2014; Higginbotham et al., 2016; Hu et al., 1986; Lundegaard et al., 2009; Parker et al., 1996; Pickard and Needs, 2010; Polsin et al., 2017; Zha and Boehler, 1985) is evolving: it includes descriptions of the exciting electride phases, improved understanding of the geophysics of planetary bodies including exoplanets (Wang et al., 2013; McMahon and Nelmes, 2006; Ping et al., 2013; Belonoshko, 1994), advanced construction of engineering structures in extreme thermal environments (LeBlanc et al., 2021; Yehia and Kashwani, 2013) or in high stress applications from A to Z i.e., aluminum alloyed with lithium to zirconia stabilized with yttria and all the microstructural designs of lightweight yet strong meta-materials (Berger et al., 2017; Berger et al., 2018; Milton, 2018; Hashin and Shtrikman, 1963; Kadic et al., 2019).

Over 70 years ago there was a series of papers that investigated the hypothesis that the elastic, shear moduli of solids were only dependent on the specific volume (Kê, 1949; Lazarus, 1949). Both papers concluded that the thermodynamic experimental evidence, at that time, did not support the hypothesis. The analyses used were based on thermodynamics with the state variables of pressure, p, absolute temperature, T, and specific volume, v. The thermodynamic analyses thus explicitly excluded all shear stresses, τ, as relevant mechanical state variables. The state variable τ and its thermodynamic conjugate shear strain, γ are state variables needed to define the shear modulus. More recently, the thermal analysis (Ledbetter, 2006) of sound speed data obtained using the moduli of copper repeated the conclusions of (Kê, 1949; Lazarus, 1949) again no shear variables were included. Although, thermodynamic terms found in the analysis (Ledbetter, 2006) were comparable, they did not exactly cancel. Again, the p, v and T data without τ did not support the hypothesis that v is the only state variable in the sound speed in copper. The equations for the longitudinal sound speed include contributions from the shear modulus. Thermodynamic analysis of shear moduli without shear included as a relevant state variable will have limited value.

Equation of state, EOS, tables (Lyon, 1992) describing a very wide

* Corresponding author.
E-mail address: stephen.j.burns@rochester.edu (S.J. Burns).

https://doi.org/10.1016/j.ijsolstr.2023.112347
Received 7 December 2022; Received in revised form 16 May 2023; Accepted 25 May 2023
Available online 30 May 2023

selection of materials include: *T, p, v*, and internal energy variables are curated at Los Alamos National Laboratory. These tables are constructed from measured physical properties using Helmholtz's free energy; solid materials are included in the low *T* part of the tables. These EOS do not include any shear varibles in describing solids and generally are used to describe gasses and liquids. Descriptions of material properties at high strain-rates and extensive *T* ranges were recently reviewed in Armstrong (2021). These models of solids are solely based on shear stress deformation and are thus excluded from EOS table descriptions.

Swenson's law (Swenson, 1968; Monfort and Swenson, 1965; Anderson, 1995; Anderson and Anderson, 1970; Anderson, 1979) hypothesized that the isothermal, bulk elastic moduli are independent of *T* and *p* at constant *v*. This law is considered to be very widely applicable by Anderson (1995); the opposite conclusion is reached by Lawson and Ledbetter (2011) based on a through and complete *p, v*, and *T*, but no τ, thermal analysis. Swenson's law if corroborated would support the hypothesis and evidence in Kê (1949), Lazarus (1949), Ledbetter (2006) since the modulus only depends on *v*. This concept is explored below by expanding the independent mechanical state variables in elastic solids to include τ directly as a state variable. The τ state variable is obtained by a rotation of the Cauchy stress tensor in a solid. The thermodynamics then explicitly includes both *p* and τ as mechanical descriptions for the elastic solid.

Observations that seem to have unconnected origins are an important aspect of the physical properties described above. Consider: Gibson and Ashby 1982 working with a foam who called their relation between modulus and density a 'scaling-law' with the power exponent between 2 and 3 for open and closed cell foams respectively (Gibson and Ashby, 1982; Ashby and Medalist, 1983; Ashby, 2005; Huber, 2018); O. L. Anderson 1967 discovered a volumetric relation with thermal expansion which is dependent on the 'Anderson-Grüneisen exponent' with the exponent typically about 5 for fully dense solids (Anderson, 1967; Reynard and Price, 1990; Anderson et al., 1992; Barron, 1979); Burns (2018a, 2018b) related the elastic shear compliance to the specific volume using thermodynamics and called his relation a 'constitutive-law'; Birch (1938) and then Murnaghan (1944) noted that an 'Equation of State' found by Birch-Murnaghan can be reduced to a simple power-law relating the modulus to the density through a power-law in most cases. Grover et al. (1973) called their semi-logarithmic form of the moduli versus the dilatation a 'Simple Compressibility Relation for Solids' and applied it to over 70 solids. Mast (2000) empirically related the wave speed in human tissue to the density. This relation is used in Boyd et al. (2010) to ultrasonically detect cancers in women's breasts. Finally, the elastic relation for graphene, man-made metamaterials at the limits of Hashin-Shtrikman structures and 2-dimensional Schneebeli materials are described by a power-law (Qin et al., 2017; Hall et al., 2010). Tallon and his co-authors (Tallon et al., 1977; Tallon, 1979; Tallon and Wolfenden, 1979; Tallon, 1980; Tallon, 1982) explored Born-Durand-Tallon theory of melting in aluminum single crystals. They used Grover, et al. 1973 semi-logarithmic moduli versus dilatation relation while including phase co-existence between the solid and the melt. Tallon also reported on the elastic moduli of 42 materials in a semi-log description with isobaric dilatation using Murnaghan's 1944 expressions. Tallon 1980 used Swenson's law for the elastic moduli and Grüneisen's parameter to describe the product of moduli with the dilatation but having little or no dependence on *T* nor *p*. It seems that a law relating the elastic moduli to the specific density or dilatation is empirically well established and has some theoretical basis; this concept is expanded on below using the shear variables in solids.

No distinction is generally made between the isothermal, μ_T and the isentropic μ_S shear moduli. *S* is the entropy in the shear modulus subscript. Shear stress-wave speeds for over a century, have not been corrected for thermal effects because the shear thermal expansion is always considered to be zero except for (Burns, 2018b) and (Porporato et al., 2019). The presumption of no shear thermal expansion negates the necessity to consider heat; there is no temperature change, so there should be no heat to equilibrate.

Our research shows that elastic moduli are power-law functions of the specific volume whether the change in specific volume comes from thermal or pressure changes, or any combination of both. We have added a shear variable to the thermodynamic analyses noted above that leads us to this conclusion. The shear stress and pressure are the independent mechanical state variables in an expanded thermodynamic system. We start by first considering an octahedral stress tensor to represent pressure plus effective shear stresses. Thermodynamics is then developed by consideration of the shear thermal expansion coefficient to establish the consequences for this system. Finally, we provide additional experimental evidence of the moduli-dilatation as a power law.

2. Cauchy's stress tensors in solids

Eq. (1) is a general stress tensor in a solid.

$$\tilde{\sigma}\Rightarrow\begin{pmatrix}\sigma_{xx} & \tau_{xy} & \tau_{xz}\\ \tau_{xy} & \sigma_{yy} & \tau_{yz}\\ \tau_{xz} & \tau_{yz} & \sigma_{zz}\end{pmatrix}\Rightarrow\begin{pmatrix}\sigma_{11} & 0 & 0\\ 0 & \sigma_{22} & 0\\ 0 & 0 & \sigma_{33}\end{pmatrix}\Rightarrow\begin{pmatrix}\sigma_{1'1'} & \tau_{1'2'} & \tau_{1'3'}\\ \tau_{1'2'} & \sigma_{1'1'} & \tau_{2'3'}\\ \tau_{1'3'} & \tau_{2'3'} & \sigma_{1'1'}\end{pmatrix} \tag{1}$$

A stress tensor with normal stresses σ and shear stresses τ in equilibrium is symmetric about the diagonal so the first tensor may always be rotated to the principal stresses and principal coordinates as seen by the second tensor in expression (1). The stress state is the same in the third tensor: a rotation, as explained below, is used to find this tensor. The rotation axis in Fig. 1 lies in the 2–3 plane with the rotation being at equal angles to 2 and 3 axes; 1 is rotated through an angle ψ. This new rotated axis is called $1'$ and is equidistance from 2 and 3. The axes 2 and 3 are also rotated with the ψ rotation and become $2'$ and $3'$ respectively. The angle ψ is chosen so the normal stress on the $1'$ face is equal to 1/3 of the trace of the stress tensor. The third tensor shows all the normal stresses, $\sigma_{1'1'}$, $\sigma_{2'2'}$ and $\sigma_{3'3'}$ are equal in the octahedral stress state (Chen and Saleeb, 1982; Chen and Han, 2007) and the shear stresses for this face are proportional to the deviatoric stresses in Eq. (1):

$$\tau_{1'2'}=\frac{1}{3}(\sigma_{11}-\sigma_{22});\ \tau_{2'3'}=\frac{1}{3}(\sigma_{22}-\sigma_{33});\tau_{1'3'}=\frac{1}{3}(\sigma_{33}-\sigma_{11}) \tag{2}$$

This octahedral stress state is well described in the literature but is not used extensively as maximum shear stress systems are dominant. There are a total of 8 octahedral planes: the perpendicular normal from the 8 planes are at an angle of 54.736 degrees with the principal stress axes.

3. Energy balances in the pressurized and sheared thermodynamic system

The incremental energy balance per unit mass from the 1st law of thermodynamics for the stress state shown on the far right side of expression (1) is:

$$du=TdS+v\sigma_{i'i'}d\varepsilon_{i'i'}+v\tau_{1'2'}d\gamma_{1'2'}+v\tau_{1'3'}d\gamma_{1'3'}+v\tau_{2'3'}d\gamma_{2'3'} \tag{3}$$

The first term on the left, *du*, is the incremental internal energy of the system per unit mass. On the right side *T* is the temperature; *S* is the entropy per unit mass; *TdS* is the incremental heat add to the system. *v* is the specific volume i.e., volume per unit mass. $v\sigma_{i'i'}d\varepsilon_{i'i'}$ is the incremental mechanical work per unit mass done on the i' surface due to the normal stress. $\sigma_{1'1'}$ is the normal stress on the $1'$ plane and $\varepsilon_{1'1'}$, $\varepsilon_{2'2'}$ and $\varepsilon_{3'3'}$ are the normal strains in the $1'$, $2'$ and $3'$ directions respectively. $v\tau_{i'j'}d\gamma_{i'j'}$ is the incremental mechanical work per unit mass due to the shear stresses, $\tau_{i'j'}$. γ_{ij} is the corresponding engineering strain. $\tau_{1'2'}$ is the shear stress on the $1'$ face in the $2'$ direction as shown in Fig. 1(b). Eq. (3) shows all three shear terms for the $1'$, 2' and 3' faces. In Eq. (3) the trace of the normal strains are well known:

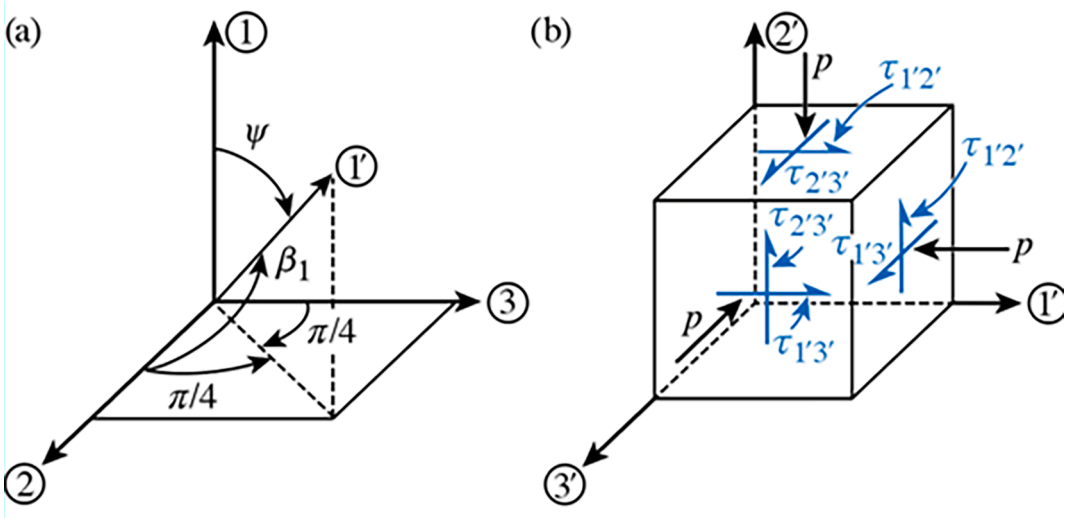

Fig. 1. (a). Rotation of the 1 axis, in the principal coordinate system, is through the angle ψ. The rotation is about a line that lies in the 2 −3 plane at 45 degrees to both axes. $\psi = 54.736°$. (b). Shows the stresses on the rotated stress cube with normal stresses as -p and τ stresses displayed.

$$d\varepsilon_{1'1'} + d\varepsilon_{2'2'} + d\varepsilon_{3'3'} = \frac{dv}{v} \tag{4}$$

So with this substitution and

$$\sigma_{1'1'} = -p = \frac{1}{3}(\sigma_{11} + \sigma_{22} + \sigma_{33}) \tag{5}$$

We now have for (3)

$$du = TdS - pdv + v\tau_{1'2'}d\gamma_{1'2'} + v\tau_{1'3'}d\gamma_{1'3'} + v\tau_{2'3'}d\gamma_{2'3'} \tag{6}$$

The shear strain-volume (Li, 1978; Burns, 2011) is defined in incremental form using the symbol $\underline{\gamma_{ij}}$.

$$vd\gamma_{ij} \equiv d\underline{\gamma_{ij}} \tag{7}$$

The strain-volume definition places no restriction on v. It allows u to be transformed from the internal energy to the Gibbs' like free energy, g, while maintaining energy per unit mass. g is a free energy with complimentary work terms that use Eqs. (6) and (7):

$$g = u - TS + pv - \tau_{1'2'}\underline{\gamma_{1'2'}} - \tau_{1'3'}\underline{\gamma_{1'3'}} - \tau_{2'3'}\underline{\gamma_{2'3'}}. \tag{8}$$

In incremental form, we have from Eqs. (6) through (8):

$$dg = -SdT + vdp - \underline{\gamma_{1'2'}}d\tau_{1'2'} - \underline{\gamma_{1'3'}}d\tau_{1'3'} - \underline{\gamma_{2'3'}}d\tau_{2'3'} \tag{9}$$

A constitutive or single effective shear stress based on Eq. (2) is employed here to reduce the three shear stresses to a single representative shear term in the Gibbs' like incremental free energy function, (9). This shear stress is neither a von Mises nor a Tresca stress; it is the effective octahedral shear stress which is proportional to a von Mises shear stress. Separation of the system into pressure and shear allows the material to have shear deformation while holding p constant or hold shear constant and allow for p changes. The octahedron changes v with pressure but not shape and shear strain changes shape but not v. The shear stress in Eq. (10) is based on distortional strain energies acting on the octahedron.

$$\begin{aligned}\tau_0 &= \sqrt{\frac{1}{3}\left((\tau_{1'2'})^2 + (\tau_{1'3'})^2 + (\tau_{2'3'})^2\right)} \\ &= \frac{1}{3}\sqrt{(\sigma_{11} - \sigma_{22})^2 + (\sigma_{33} - \sigma_{11})^2 + (\sigma_{22} - \sigma_{33})^2}.\end{aligned} \tag{10}$$

And the effective shear strain-volume is:

$$\underline{\gamma_0} = \frac{1}{3}\left(\underline{\gamma_{1'2'}} + \underline{\gamma_{1'3'}} + \underline{\gamma_{2'3'}}\right) \tag{11}$$

The last three incremental complimentary energy terms on the right in Eq. (9) are now replaced with single effective shear so the Gibbs' like energy function from the last tensor in expression (1) is:

$$dg = -SdT + vdp - 3\underline{\gamma_0}d\tau_0 \tag{12}$$

4. Thermodynamic property definitions in the shear system only

The Gibbs free energy in thermodynamic systems described with p and v as the mechanical variables are well known in the literature including several books. In what follows below, the thermodynamic mechanical variable is only shear stress and shear strain restricted to an isobar. Thus, the mechanical system variables of τ_0 and γ_0 which describes the physical shear properties are unique to sheared solids and are explored below in detail. Eq. (12) when restricted to an isobar is:

$$dg = -SdT - 3\underline{\gamma_0}d\tau_0 \tag{13}$$

We see from Eq. (13) that:

$$\left.\frac{\partial g}{\partial T}\right|_{\tau_0} = -S\,;\ \left.\frac{\partial g}{\partial \tau_0}\right|_{T} = -3\underline{\gamma_0} \tag{14}$$

and from Eqs. (7) and (14), we obtain a Maxwell relation:

$$\frac{\partial^2 g}{\partial \tau_0 \partial T} = -\left.\frac{\partial S}{\partial \tau_0}\right|_{T} = -3v\left.\frac{\partial \gamma_0}{\partial T}\right|_{\tau_0} = \frac{\partial^2 g}{\partial T \partial \tau_0} \tag{15}$$

The middle expression in (15) is a differential expression for the entropy from the shear stress.

$$dS = 3v\left.\frac{\partial \gamma_0}{\partial T}\right|_{\tau_0} d\tau_0. \tag{16}$$

The thermal expansion coefficients in shear are very different from thermal expansion coefficients in the normal strains found with p, v and T state variables. Consider the physical differences seen in Fig. 2. In this figure both normal strains and shear strains are shown. The schematic shows the thermal derivatives of both strains at constant stress, but not necessarily at zero stress, as is frequently assumed. Solids with an applied shear stress will change shape upon heating as seen in Fig. 2(a) in panels (iii) and (iv) as explained below. Without the application of a shear stress the solid shows no thermal shape changes. This physical

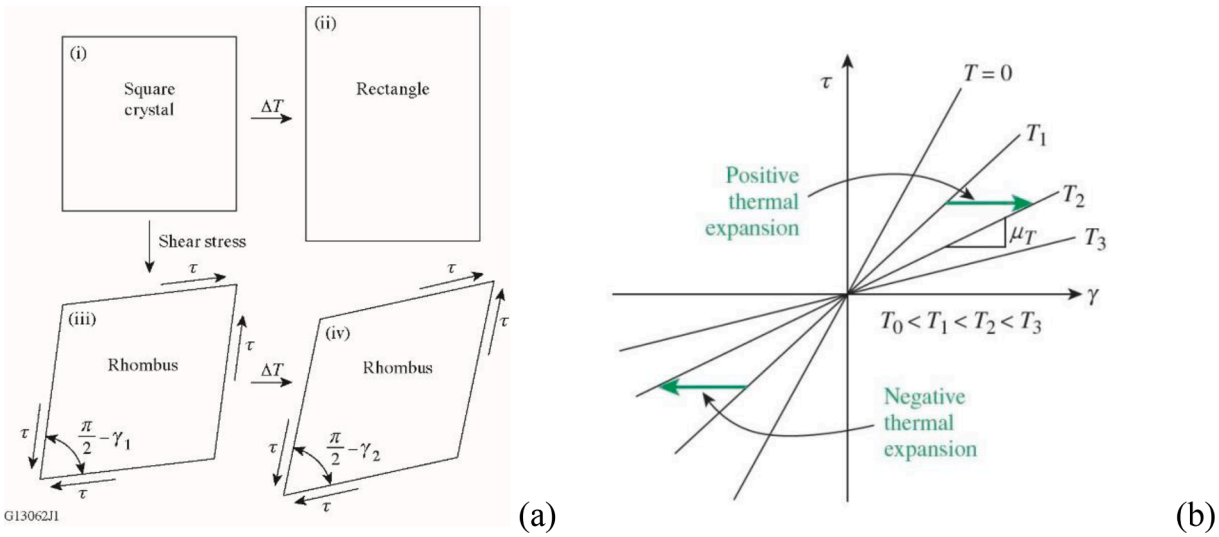

Fig. 2. (a). A schematic of thermal principal strains seen in material with and without applied shear stress. The first panel (i) is a square in a crystal; the second panel marked (ii) after heating is a rectangle; the third panel with the application of shear stress marked (iii) is a rhombus; the last panel marked (iv) is a rhombus with a more acute shear-strain angle. (b) A schematic showing isothermal, linear-elastic, shear-stress, τ, versus shear-strain, γ, on isotherms. All the isotherms cross at the point (0, 0). The shear thermal expansion is marked in green and μ_T is the shear modulus or the reciprocal compliance.

difference leads to equations of state that are unfamiliar to well-known equations of state in the p, v and T systems.

Fig. 2(a) shows material schematically in the first panel labeled (i) on the left at a temperature T_0. The square is then heated with a temperature change of ΔT. The material will expand due to thermal expansion. The original square is now displayed in the general case as a rectangle on the second upper panel (ii) of the schematic. The material does not change shape if it is incrementally heated using the principal coordinates of Eq. (1). Fig. 2(a) shows in the lower left panel (iii) the application of a shear stress, one of the three independent shear stresses, which causes material to change shape. The square is now a rhombus. Panel (iii) shows the shape change due to the mechanical application of the shearing stress. Upon heating by ΔT the shape again changes as seen in the lower right panel (iv) with a larger shear strain; it becomes a more acute rhombus; the same result is seen in Fig. 2(b) as the shear thermal expansion coefficient follows the green arrow. The application of shear stress is the source of the shear thermal expansion coefficients which are zero when the shear stress is zero as seen in Fig. 2(b). The third quadrant shows negative shear thermal expansion coefficients with negative shear stresses.

The shear thermal expansion coefficient is the thermal part of the shear strain. It is well known that solids support shear stresses, τ_0 and engineering shear strains, γ_0 as seen below in the linear Eq. (17). λ_T is the linear, isothermal, shear compliance.

$$\gamma_0 = \lambda_T \tau_0 \tag{17}$$

The temperature derivative of the shear strain as shown in Fig. 2 (b) and from Eq. (17) is the shear thermal expansion coefficient as

$$\left.\frac{\partial \gamma_0}{\partial T}\right|_{\tau_0} = \tau_0 \left.\frac{\partial \lambda_T}{\partial T}\right|_{\tau_0} \tag{18}$$

Generally, all other stresses are held constant.

Substitution from Eq. (18) in a linear system, into Eq. (16) and integration with T constant as dictated by the middle-left side of Eq. (15) allows for integration and yields S for linear elastic systems.

$$S = \int_0^{\tau_0} 3v\tau_0 \left.\frac{\partial \lambda_T}{\partial T}\right|_{\tau_0} d\tau_0 = 3v\frac{\tau_0^2}{2}\left.\frac{\partial \lambda_T}{\partial T}\right|_{\tau_0} \tag{19}$$

A constant S curve in τ versus γ space is obtained from knowledge of the T dependence of λ_T. This is seen by solving Eq. (19) for τ with S constant; it yields:

$$\tau_0 = \left(\frac{2S}{3v\left.\frac{\partial \lambda_T}{\partial T}\right|_{\tau_0}}\right)^{1/2}. \tag{20}$$

And with the aid of Eq. (17), we find:

$$\gamma_0 = \lambda_T \left(\frac{2S}{3v\left.\frac{\partial \lambda_T}{\partial T}\right|_{\tau_0}}\right)^{1/2} \tag{21}$$

The T dependence of λ_T, $\left.\frac{\partial \lambda_T}{\partial T}\right|_{\tau_0}$ and a fixed value for S, yields a parameterized curve of τ_0 versus γ_0 with entropy constant from Eqs. (20) and (21).

Fig. 3 is data (Simon et al., 1992; Ledbetter and Naimon, 1974) for the T dependence of the shear compliance, λ_T, of polycrystalline copper. The measured data was the shear modulus, μ_T, which is used below to

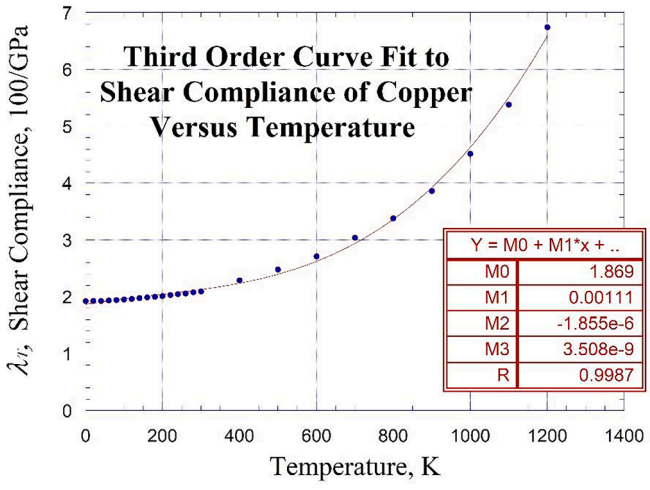

Fig. 3. Shear compliance of copper versus T. A third order curve fit to the data is shown. The original data is from references (Simon et al., 1992; Ledbetter and Naimon, 1974). Copper melts at 1357 K.

construct an adiabatic line in a two-independent-variable thermodynamic system; it assumes a simple third order power law series in T to describe the temperature dependence of λ_T. Fig. 3 shows $\lambda_T = 1/\mu_T$ versus T from two sets of measurements of shear modulus of copper cited above. These two different measurements were matched at $T = 300$ K. The higher T values have been corrected with the ratio of the match at $T = 300$ K which results in a smooth curve. The curve fit to the data in Fig. 3 was used to construct the T dependence of λ_T and $\partial\lambda_T/\partial T|_{\tau_0}$ in the parametric expressions for the constant entropy curve.

Fig. 4 is a construction of the constant entropy curve using equations (20) and (21). The isentropic slope of Fig. 4 versus T is plotted in Fig. 5. This slope is the isentropic shear modulus, μ_S i.e., the slope of the constant S curve. The isothermal shear modulus, μ_T, taken from the original data is also given for comparison in Fig. 5.

The thermodynamic relation that connects the isothermal and isentropic shear moduli is found from Table 1 using Jacobian algebra and is given in expression (T-2).

$$\lambda_S = \lambda_T - 3\nu\frac{T}{C_{\tau_0}}\left(\tau_0\frac{\partial\lambda_T}{\partial T}\bigg|_{\tau_0}\right)^2 \tag{22}$$

The constant shear stress heat capacity C_{τ_0} is for a shear only stress system. It is included in Table 1. C_{τ_0} is found with the aid of Eq. (19) and Table 1; it is listed as expression (T-3). Using this expression for the heat capacity the following differential Eq. is found from Eq. (22) with the primes as the first and second derivatives:

$$\lambda_S = \lambda_T\left(1 - 2\frac{\left(\lambda_T'\right)^2}{\lambda_T\lambda_T''}\right) \tag{23}$$

5. A universal law for the volume dependence of the shear modulus

The isothermal lines must exist at the zero-stress crossing in Figs. 2 (b) and 5. The requirements are for all isothermal crossings to have no second-law violations, no temperature changes in the sheared solid except through ν, and keep μ_s proportional to μ_T so a solid can be rapidly sheared without changing temperature on crossing through the zero-thermal expansion coefficient point. This form is possible if the differential Eq. on the right side of Eq. (23) is satisfied for the adiabatic lines at the isothermal crossing point and throughout the shear-stress, shear-strain space. The T derivatives of the shear compliance will not allow for these conditions as seen in Figs. 4 and 5. The differential equation below from the right of Eq. (23) describes the slope of adiabatic stress versus

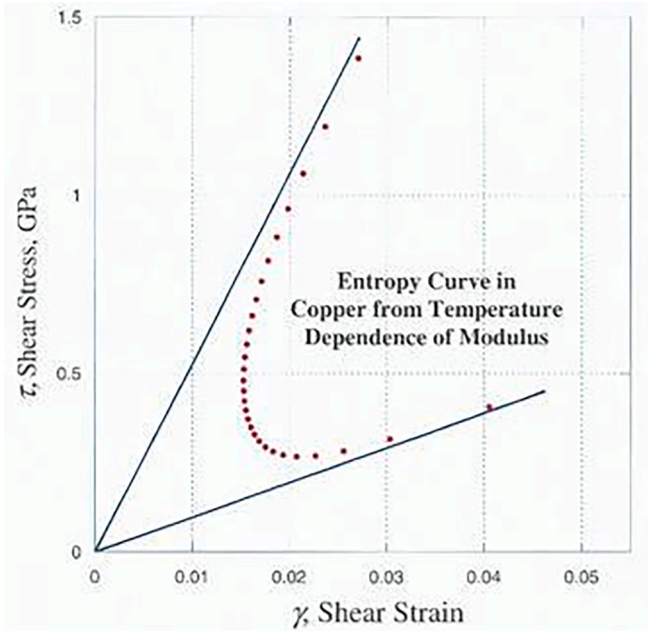

Fig. 4. The shear stress versus shear strain on a constant entropy curve bounded between two isotherms is displayed. The mirror image is in the 3rd quadrant. S was chosen as 3.3 J/mole*K, the density of copper was taken as 8.96 gm/cm^3 and the atomic weight as 63.55 au. Eqs. (20) and (21) plus the curve fit data from Fig. 3 are used for the construction of the dotted curve. The two solid blue lines are isothermal asymptotes.

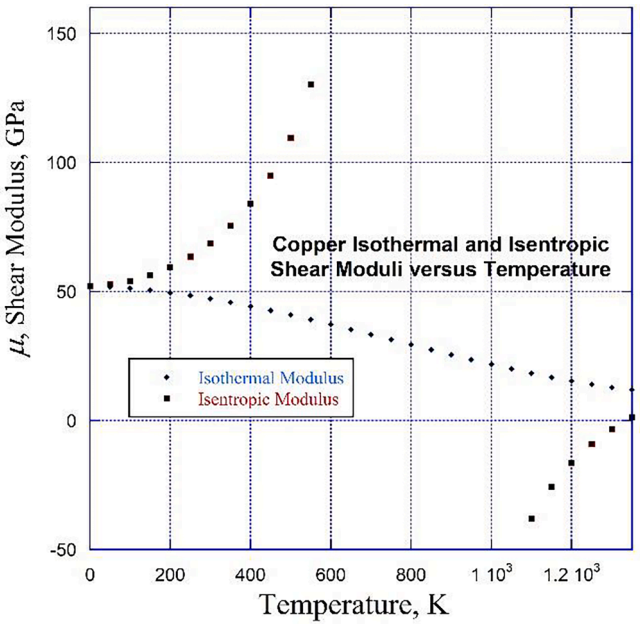

Fig. 5. The measured isothermal shear modulus and the isentropic shear modulus constructed from the slope of the constant entropy curve in Fig. 4. The isothermal data are shown as diamonds and isentropic moduli are plotted as squares, both are shown versus T.

Table 1
A table constructed to describe the thermodynamic system in Eq. (13). The Table is in Jacobian format and contains the physical properties and Maxwell's Eq. (15) for the system. The system is restricted to linear shear elasticity in Eq. (17). All partial derivatives may be found using Jacobian algebra and Table 1's entries. See Eq. (T-1) and (T-2) displayed below Table 1 for examples.

function	$\frac{\partial}{\partial T}\big\|_{\tau_0}$	$\frac{\partial}{\partial \tau_0}\big\|_{T}$
Temperature, T	1	0
Effective shear stress, τ_0	0	1
System entropy, S	$\frac{C_{\tau_0}}{T}$	$3\nu\tau_0\frac{\partial\lambda_T}{\partial T}\big\|_{\tau_0}$
Effective shear strain, γ_0	$\tau_0\frac{\partial\lambda_T}{\partial T}\big\|_{\tau_0}$	λ_T

$$\frac{\partial\gamma_0}{\partial\tau_0}\bigg|_S \equiv \lambda_S = \frac{J(\gamma_0,S)}{J(\tau_0,S)} = \frac{\begin{vmatrix} \tau_0\frac{\partial\lambda_T}{\partial T}\big|_{\tau_0} & \lambda_T \\ C_{\tau_0}/T & 3\nu\tau_0\frac{\partial\lambda_T}{\partial T}\big|_{\tau_0}\end{vmatrix}}{\begin{vmatrix} 0 & 1 \\ C_{\tau_0}/T & 3\nu\tau_0\frac{\partial\lambda_T}{\partial T}\big|_{\tau_0}\end{vmatrix}} = \lambda_T - 3\nu\frac{T}{C_{\tau_0}}\left(\tau_0\frac{\partial\lambda_T}{\partial T}\bigg|_{\tau_0}\right)^2. \text{ (T-1)}$$

$$\lambda_S = \lambda_T - 3\nu\frac{T}{C_{\tau_0}}\left(\tau_0\frac{\partial\lambda_T}{\partial T}\bigg|_{\tau_0}\right)^2. \text{ (T-2)}$$

C_{τ_0} is obtained by using Eq. (19) in the S line of Table 1.

$$C_{\tau_0} = 3\nu T\frac{\tau_0^2}{2}\frac{\partial^2\lambda_T}{\partial T^2}\bigg|_{\tau_0}. \text{ (T-3)}$$

strain curve at all points in the entire τ vs γ space. Take the shear compliance to be $\lambda(v)$ and primes on λ are derivatives with respect to v so the adiabatic slope is proportional to the isothermal slope. The shear compliance is not the same as λ_T since elastic compliances are in general considered functions of the thermodynamic variables. λ is considered only as a function of v which avoids the difficulties seen in Fig. 5. The numerical values of λ_S and λ_T are identical with $\lambda = \lambda(v)$. Eq. (23) with these restrictions implies:

$$\frac{(\lambda')^2}{(\lambda)(\lambda'')} = \text{constant} \tag{24}$$

The general solution to the second-order differential Eq. (24) with both integration constants is evaluated in Supplemental Material A as Eq. (A-12). The solution in (25) is after application to a reference state to evaluate the arbitrary constants of integration:

$$\frac{\lambda}{\lambda_0} = \left(\frac{v}{v_0}\right)^m \lambda = C_0 v^m \text{ or } \mu = \frac{\rho^m}{C_0} \tag{25}$$

v is the specific volume, v_0 is a reference specific volume at the same reference state as the shear compliance, λ_0; ρ is the density and μ which only depends on v is Lame's second shear modulus and is now only a function that depends on v i.e., a specific volume line. v in turn is a function of the pressure p and T and all other thermodynamic variables. C_0 is a constant formed from the reference states. Eq. (25) is the solution to the differential Eq. (24) for a constant on the right side. Eq. (25) contains m a constant on the right from Eq. (24) or Eq. (A-12); the two constants of integration are already explicitly given in (A-12) and Eq. (25).

5.1. Elastic constants dependence on the specific volume

The argument to mandate all elastic constants only dependent on specific volume is based on the transformation laws of elastic constants in one orientation to elastic constants in a second rotated coordinate system i.e., the *state of stress* in a tensor stress field from reference (Nye, 1964; Wallace, 1972). Rotations depend on the direction cosines between the two coordinates systems and the other elastic constants. In isotropic materials a $\pi/4$ coordinate rotation is well known to relate the shear modulus in the rotated coordinate system to Young's modulus, E, and Poisson's ratio, υ, in a uniaxial stress state. E is obtained from the uniaxial stress versus uniaxial strain and Poisson's ratio which is the uniaxial strain proportioned to the negative strain on a stress-free perpendicular coordinate.

$$\mu = \frac{E}{2(1+\upsilon)} \tag{26}$$

Generally, E and υ are considered as functions of T, p and other thermodynamic variables. However, Eq. (25) has established that the shear modulus is only a function of v.

$$\mu(v); v = v(T,p) \tag{27}$$

Expression (26) with (27) shows the left side of (26) is only a function of a single variable, v, and the right side is generally considered a function of all the thermodynamic variables including T and p in both E and υ. The *state of stress* requires that both sides of (26) be functions of the same variable or variables and not be dependent on the choice of the coordinate system. The isotropic solid described in (26) on both sides is independent of the choice of coordinates. The condition for the moduli transformation to be valid is

$$E = E(v) \text{ and } \upsilon = \upsilon(v) \tag{28}$$

It follows that elastic stiffnesses and the elastic compliances are therefore not thermodynamic functions but like the shear modulus, they must be functions only of the specific volume. They can't be thermodynamic expressions dependent on additional variables. Stresses are tensors so equations (26) through (28) follow for solids and describe the transformations of both elastic stiffnesses and compliances. Elastic moduli in crystals and the effective moduli in solids and complex microstructures should be functions of the specific volume. Empirical support of this statement is given below while earlier references (Gibson and Ashby, 1982; Ashby and Medalist, 1983; Ashby, 2005; Huber, 2018; Anderson, 1967; Reynard and Price, 1990; Anderson et al., 1992; Burns, 2018; Burns, 2018; Birch, 1938; Murnaghan, 1944; Grover et al., 1973; Mast, 2000; Qin et al., 2017; Hall et al., 2010; Tallon et al., 1977; Tallon, 1979; Tallon and Wolfenden, 1979; Tallon, 1980; Tallon, 1982) have, as already noted, moduli that depends only on v.

6. Empirical evidence to support the specific volume dependence of the elastic moduli

Empirical evidence will now be presented in support of Eq. (25). The first materials are with shear moduli data of metals, ceramics and minerals. Fig. 6 throughout uses relative values for both the elastic shear compliances and volumes. The investigation on copper used the T dependence of λ_T and v in Eq. (25) in parametric form. Fig. 6 is a plot of $\ell n(\lambda_T)$ versus $\ell n(v)$ for oxygen-free copper. The assumption in the data is that $\mu_s = \mu_T = \mu$. The data were taken from reference (Simon et al., 1992; Ledbetter and Naimon, 1974). Each point in this plot is at a different T or p. The data are from very low temperatures near 5 K to about 300 K. Thus, all quantum effects at low temperatures are included in the data presented. v in the data used in Fig. 6 is from numerical integration of 3 times the measured linear thermal expansion coefficient. The measurements were obtained from the same copper rod.

MgO single crystal measurements (Isaak et al., 1989; Li et al., 2006) are the second material in Fig. 6 that was chosen for study. The data are for thermal changes for a cubic single crystal's elasticity. The single crystal shear compliance S_{44} scale is also on the left of the graph. The temperature goes from $T = 300$ K to $T = 1{,}800$ K. The shear-compliance S_{44} versus volume with pressure as a parameter is also shown in Fig. 6.

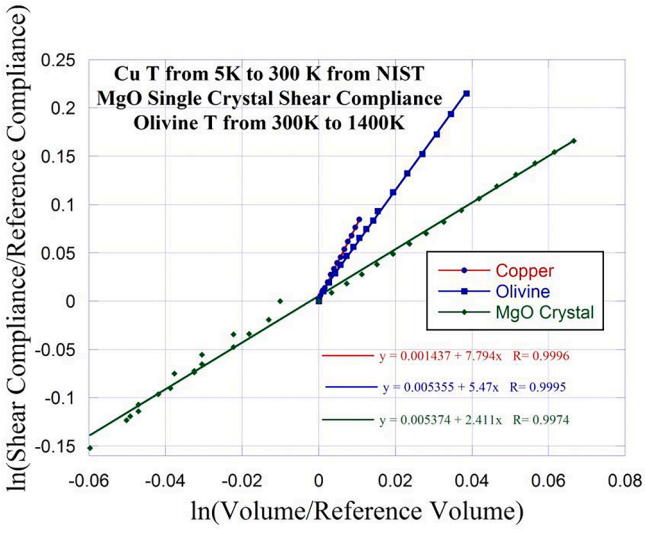

Fig. 6. Experimental shear compliances for Copper, Olivine ($Fo_{92}Fa_8$) and single crystal MgO plotted as ℓn(shear compliance/reference compliance) versus ℓn(volume/reference volume). The MgO single crystal's shear compliance is S_{44}. Data in the first quadrant use T as a parameter with each point at a different T value. The data for MgO in the third quadrant are with different pressures at each point. The data are from references (Simon et al., 1992; Ledbetter and Naimon, 1974; Isaak and Goto, 1989; Li et al., 2006; Anderson et al., 1992). Low temperature data for Cu is well below the Debye temperature. For Olivine (Anderson et al., 1992) the shear modulus at 1,000 K was taken as 69.17 GPa being between 70.54 and 67.81 GPa, the neighboring points. The table lists this value as 59.17 GPa, an assumed typographical error.

The elastic properties in compression were measured by Brillion spectroscopy in a sample within a diamond anvil cell. The material in the volume data and in the shear modulus data is from the same single crystal (Li et al., 2006). Fig. 6 shows a plot of $\ell n(S_{44})$ verus $\ell n(v)$ using parametric p and T values in the elastic shear compliance, S_{44} and v. The density comes from X-ray measurements of interatomic plane spacings. Fig. 6 on the left scale uses relative values with a slightly different reference state between the thermal and pressure data. This pressure data is in excellent agreement with the thermal data as noted above. The pressure data have significantly more scatter than the more precise thermal data. Also, increasing the temperature increases v while increasing the pressure decreases v. This is seen by having the temperature data in the 1st quadrant and the pressure data in the 3rd quadrant in the plot as is physically expected for v.

Olivine is the third material chosen for shear modulus investigation. The plot in Fig. 6 is of $\ell n(\lambda/\lambda_0)$ verus $\ell n(v/v_0)$ again with T as a parametric variable. The data for this mineral were taken from reference (Anderson et al., 1992). The temperature goes from 300 K to 1,400 K. The material used in the v data and in the shear compliance data are again the same material. Olivine is a two-phase material within a solid-solution phase field.

Fig. 7(a) and 7(b) are graphs of the elastic compressibility or the reciprocal bulk modulus of materials versus specific volume. Again, the linear fit to the measured data all have R values of 0.997 or better. The implication is that the dilatational components of the Cauchy stress tensor empirically follows Eq. (25). Fig. 7 also contains graphs of other minerals and metals.

The restriction on Eq. (25) is that the solid must support a shear stress. The solution to expression (24) would apply to all material selections with very different nano, micro or macro structures. The recent designs of material structures considered to be very stiff yet extremely light weight are reported (Berger et al., 2017, 2018). Metamaterials, engineered foams structures with both open and closed structures, graphene mats with fiber structures, etc. all seem to be described by Eq. (25). Fig. 8 is a plot of the log natural of 1/(effective shear modulus) versus the log natural of the volume from reference (Berger et al., 2017) data. The graph is the meta-structures of: Cubic foams, Octet foams, Cubic + Octet, Cubic + Octet 2, Octet Truss, Isotropic Truss and Quasi-random foams. The meta-material foam curves have been fit as straight-line data in log–log plots with m between 1.07 and 1.28 respectively for the measured power exponents.

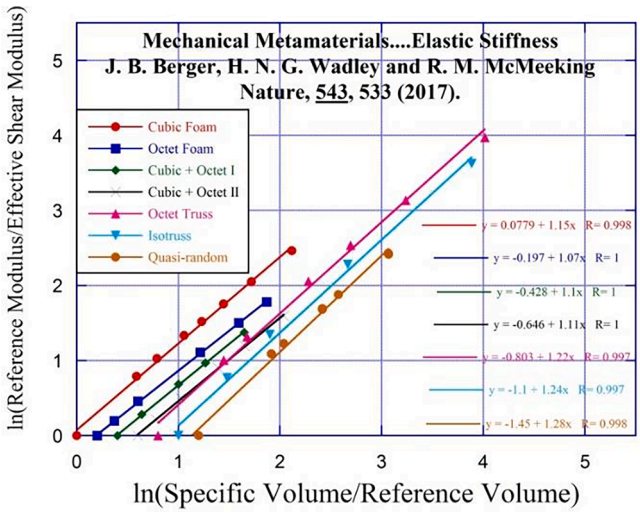

Fig. 8. Metamaterial structures analyzed with a finite element program for which representative, isothermal shear moduli and density have been determined (Berger et al., 2017). The data are plotted as ℓn(reference/shear modulus) versus ℓn(volume/reference volume). Applied strains were used as a parameter to change the internal shapes in all structures. Each color is a different metastructure curve fit to a power law relation and offset by an increment of 0.2 on the abscissa.

7. Conclusions

The use of only p, T and v as thermodynamic variables to completely describe elastic solid materials is questioned. Equations of state based only on p, v and T as descriptions for solids are quite commonplace. The reduction of all stresses in solids to the state variable of p alone ignores shear stresses. Yet solids are defined as materials that sustain shear stresses. Eq. (2) shows that with the principal stresses equal then all shear stresses are zero and the solid is the same as a thermodynamic fluid.

The universal moduli concept as derived in this manuscript comes from thermodynamics applied to a sheared elastic solid. Shear thermodynamics is unique because all the isotherms pass through the $\tau = 0$, $\gamma = 0$ point while the adiabatic lines are excluded as seen in Fig. 4. The isothermal shear stresses and shear strains pass through $\tau = 0$, $\gamma = 0$, a point that includes all isotherms and isobaric pressures but excludes the adiabatic lines. The adiabatic curves can't mimic the isotherms through this point because of second law thermodynamic considerations. This is also the point of zero shear thermal expansion coefficients at all temperatures and pressures in single crystal materials, polycrystalline materials, and structures. The material does not have to be crystalline, but it must support shear stresses i.e. is restricted to a solid without phase changes. Shear thermal expansion coefficients at zero shear stress are zero and are thus very different from normal thermal expansion

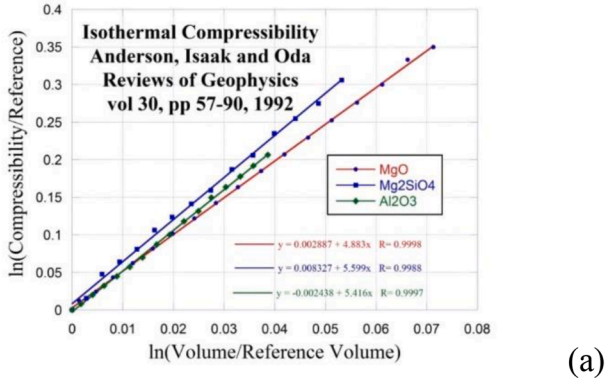

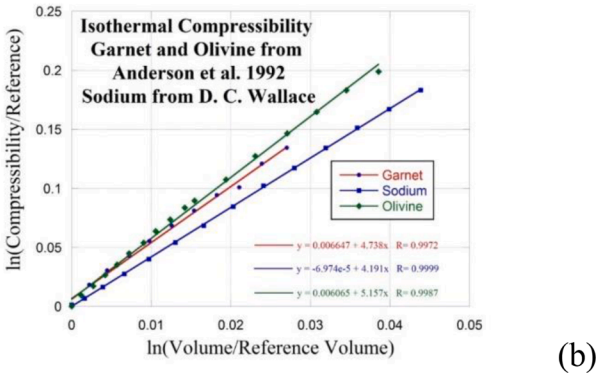

Fig. 7. (a) Experimental data of the isothermal compressibility for polycrystalline magnesia, ringwoodite and alumina (Anderson et al., 1992) plotted as ℓn(compressibility/reference compressibility) versus ℓn(volume/reference volume). (b) Experimental data of the isothermal compressibility for polycrystalline garnet, sodium and olivine (Wallace, 1972; Anderson et al., 1992) is plotted as ℓn(compressibility/reference compressibility) versus ℓn(volume/reference volume). T was used as a parameter for all plots.

coefficients. Considerations of the elastic shear moduli at all temperatures and pressures is through the material's specific density or volume. This concept is neither totally new nor unique as it was proposed in the past and quite recently only to be rejected using p, v and T thermodynamic analyses without including shear stress concepts.

Swenson's law some time ago proposed the isothermal bulk elastic moduli as having no dependence on p, and T if v is held constant. The universal Eq. (25) developed here agrees with Swenson's law while also deriving a universal form for the elastic moduli. It is argued that a single form predominates all elastic moduli: it relates the material's specific volume $v(T, p)$ to the modulus for materials in shear, $\mu(v)$. $\mu(v)'s$ thermodynamic dependence on T and p is through v. The power law descriptions were extended to all elastic moduli; the bulk moduli as developed here has consequences for materials at very high pressures which are briefly explored in the attached Supplemental Material B. The example described is one consequence of a pressurized solid via the thermodynamics explored in this text. The exponent m found initially in Eq. (25) and is seen from inspection of the empirical data presented to likely to be related to the material's packing density.

Declaration of Competing Interest

The authors declare that they have no known competing financial interests or personal relationships that could have appeared to influence the work reported in this paper.

Data availability

Data will be made available on request.

Acknowledgements

SJB would like to thank: J. C. Lambropoulos, Ranga Dias, R. M. McMeeking, J. B. Berger, D. N. Polsin, G. W. Collins, and J. R. Rygg for discussions and the Department of Energy through Basic Energy Sciences, Materials Science and Engineering who supported earlier work related to this topic. SPB would like to thank the National Center for Atmospheric Research (NCAR) which is funded through NSF. We would both like to thank a reviewer whose suggestions have greatly improved our paper.

Appendix A. Supplementary data

Supplementary data to this article can be found online at https://doi.org/10.1016/j.ijsolstr.2023.112347.

References

Anderson, O.L., 1967. Equation for thermal expansivity in planetary interiors. J. Geophys. Res. 72 (14), 3661–3668.
Anderson, O.L., 1979. The Hildebrand equation of state for minerals relevant to geophysics. Phys. Chem. Miner. 5 (1), 33–51.
Anderson, D.L., Anderson, O.L., 1970. Brief report: The bulk modulus-volume relationship for oxides. J. Geophys. Res. 75 (17), 3494–3500.
Anderson, O.L., Isaak, D., Oda, H., 1992. High-temperature elastic constant data on minerals relevant to geophysics. Rev. Geophys. 30 (1), 57–90.
Anderson, O.L., Oda, H., Isaak, D., 1992. A model for the computation of thermal expansivity at high compression and high temperatures: MGO as an example. Geophys. Res. Lett. 19 (19), 1987–1990.
Anderson, O.L., Equations of state of solids for geophysics and ceramic science. Oxford Monographs on Geology and Geophysics. Vol. 31. 1995, New York NY USA: Oxford University Press. pp. 243-274.
Armstrong, R.W., 2021. Constitutive relations for slip and twinning in high rate deformations: A review and update. J. Appl. Phys. 130 (24), 245103–245111.
Ashby, M.F., 2005. The properties of foams and lattices. Philos. Trans. R. Soc. A Math. Phys. Eng. Sci. 1838 (364), 15–30.
Ashby, M.F., Medalist, R.F.M., 1983. The mechanical properties of cellular solids. Metall. Trans. A 14 (9), 1755–1769.
Barron, T.H.K., 1979. A note on Anderson-Gruneisen functions. J. Phys. C Solid State Phys. 12 (4), L155–L159.
Belonoshko, A.B., 1994. Molecular dynamics of MgSiO3 perovskite at high pressures: Equation of state, structure, and melting transition. Geochim. Cosmochim. Acta 58 (19), 4039–4047.
Berger, J.B., Wadley, H.N.G., McMeeking, R.M., 2017. Mechanical metamaterials at the theoretical limit of isotropic elastic stiffness. Nature 543 (7646), 533–537.
Berger, J.B., Wadley, H.N.G., McMeeking, R.M., et al., 2018. Berger et al. reply. Nature 564 (7734), E2–E4.
Birch, F., 1938. The effect of pressure upon the elastic parameters of isotropic solids, according to Murnaghan's theory of finite strain. J. Appl. Phys. 9 (4), 279–288.
Boyd, N.F., Martin, L.J., Bronskill, M., Yaffe, M.J., Duric, N., Minkin, S., 2010. Breast tissue composition and susceptibility to breast cancer. J. Natl. Cancer Inst. 102 (16), 1224–1237.
Burns, S.J., 2011. Thermodynamics of the superconducting phase transformation in high Tc ceramics with magnetoelectric effects. J. Mater. Res. 4 (1), 33–38.
Burns, S.J., 2018a. 77 new thermodynamic identities among crystalline elastic material properties leading to a shear modulus constitutive law in isotropic solids. J. Appl. Phys. 124 (8), 085114–085119.
Burns, S.J., 2018b. Elastic shear modulus constitutive law found from entropy considerations. J. Appl. Phys. 124 (8), 085904–085909.
Chen, W.-F., Han, Da-Jian, Plasticity for Structural Engineers. 2007, Florida, USA: J. Ross Publishing. pp 59-84, 129-132.
Chen, W.-F. and A.F. Saleeb, Constitutive Equations for Engineering Materials. Elasticity and Modeling. Vol. 1. 1982, New York John Wiley & Sons, Inc. pp. 77-82.
Craxton, R.S., Anderson, K.S., Boehly, T.R., Goncharov, V.N., Harding, D.R., Knauer, J.P., McCrory, R.L., McKenty, P.W., Meyerhofer, D.D., Myatt, J.F., Schmitt, A.J., Sethian, J.D., Short, R.W., Skupsky, S., Theobald, W., Kruer, W.L., Tanaka, K., Betti, R., Collins, T.J.B., Delettrez, J.A., Hu, S.X., Marozas, J.A., Maximov, A.V., Michel, D.T., Radha, P.B., Regan, S.P., Sangster, T.C., Seka, W., Solodov, A.A., Soures, J.M., Stoeckl, C., Zuegel, J.D., 2015. Direct-drive inertial confinement fusion: A review. Phys. Plasmas 22 (11), 110501.
Degtyareva, V.F., 2014. Potassium under pressure: Electronic origin of complex structures. Solid State Sci. 36, 62–72.
Gibson, L.J., Ashby, M.F. 1982. The mechanics of three-dimensional cellular materials. Proc. R. Soc. London. A. Math. Phys. Sci., 382: 43-59.
Grover, R., Getting, I.C., Kennedy, G.C., 1973. Simple compressibility relation for solids. Phys. Rev. B 7 (2), 567–571.
Hall, S.A., Muir Wood, D., Ibraim, E., Viggiani, G., 2010. Localised deformation patterning in 2D granular materials revealed by digital image correlation. Granul. Matter 12 (1), 1–14.
Hashin, Z., Shtrikman, S., 1963. A variational approach to the theory of the elastic behaviour of multiphase materials. J. Mech. Phys. Solids 11 (2), 127–140.
Hicks, D.G., Boehly, T.R., Celliers, P.M., Eggert, J.H., Moon, S.J., Meyerhofer, D.D., Collins, G.W., 2009. Laser-driven single shock compression of fluid deuterium from 45 to 220 GPa. Phys. Rev. B 79 (1).
Higginbotham, A., Stubley, P.G., Comley, A.J., Eggert, J.H., Foster, J.M., Kalantar, D.H., McGonegle, D., Patel, S., Peacock, L.J., Rothman, S.D., Smith, R.F., Suggit, M.J., Wark, J.S., 2016. Inelastic response of silicon to shock compression. Sci. Rep. 6 (1).
Hu, J.Z., Merkle, L.D., Menoni, C.S., Spain, I.L., 1986. Crystal data for high-pressure phases of silicon. Phys. Rev. B 34 (7), 4679–4684.
Hu, S.X., Militzer, B., Goncharov, V.N., Skupsky, S., 2010. Strong coupling and degeneracy effects in inertial confinement fusion implosions. Phys. Rev. Lett. 104 (23).
Huber, N., 2018. Connections between topology and macroscopic mechanical properties of Three-Dimensional open-pore materials. Front. Mater. 5, 069.
Isaak, D.G., Anderson, O.L., Goto, T., 1989. Measured elastic moduli of single-crystal MgO up to 1800 K. Phys. Chem. Miner. 16, 704–713.
Kadic, M., Milton, G.W., van Hecke, M., Wegener, M., 2019. 3D metamaterials. Nat. Rev. Phys. 1 (3), 198–210.
Kê, T.-S., 1949. Analysis of the temperature coefficient of shear modulus of aluminum. Phys. Rev. 76 (4), 579.
Lawson, A.C., Ledbetter, H., 2011. Coupled temperature dependences of volume and compressibility. Philos. Mag. 91 (10), 1425–1440.
Lazarus, D., 1949. The variation of the adiabatic elastic constants of KCl, NaCl, CuZn, Cu, and Al with pressure to 10,000 Bars. Phys. Rev. 76 (4), 545–553.
LeBlanc, J., Cavallaro, P., Torres, J., Ponte, D., Warner, E., Chenwi, I., Shukla, A., 2021. Effects of water saturation and low temperature coupling on the mechanical behavior of carbon and E-Glass epoxy laminates. Int. J. Lightweight Mater. Manuf. 4 (3), 358–369.
Ledbetter, H., 2006. Sound velocities, elastic constants: Temperature dependence. Mater. Sci. Eng. A 442 (1–2), 31–34.
Ledbetter, H.M., Naimon, E.R., 1974. Elastic properties of metals and alloys. II. Copper. J. Phys. Chem. Ref. Data 3 (4), 897–935.
Li, J.-C.-M., 1978. Physical chemistry of some microstructural phenomena. Metall. Trans. A 9 (10), 1353–1380.
Li, B., Woody, K., Kung, J., 2006. Elasticity of MgO to 11 GPa with an independent absolute pressure scale: Implications for pressure calibration. J. Geophys. Res. Solid Earth 111, B11206–B11210.
Lundegaard, L.F., Gregoryanz, E., McMahon, M.I., Guillaume, C., Loa, I., Nelmes, R.J., 2009. Single-crystal studies of incommensurate Na to 1.5 Mbar. Phys. Rev. B 79 (6).
Lyon, S.P., SESAME Tables: Los Alamos National Laboratory Equation of State Database. 1992. p. LANL report: LA-UR-92-407.
Mast, T.D., 2000. Empirical relationships between acoustic parameters in human soft tissues. Acoust. Res. Lett. Online 1 (2), 37–42.
McMahon, M.I., Nelmes, R.J., 2006. High-pressure structures and phase transformations in elemental metals. Chem. Soc. Rev. 35 (10), 943–963.
Milton, G.W., 2018. Stiff competition. Nature 564 (7734), E1–E.

Monfort, C.E., Swenson, C.A., 1965. An experimental equation of state for potassium metal. J. Phys. Chem. Solid 26 (2), 291–301.
Murnaghan, F.D., 1944. The compressibility of media under extreme pressures. Proc. Natl. Acad. Sci. U.S.A. 30 (9), 244–247.
Nye, J.F., 1964. Physical Properties of Crystals. Oxford University Press, London, UK, pp. 131–149.
Parker, L.J., Atou, T., Badding, J.V., 1996. Transition element-like chemistry for potassium under pressure. Science 273 (5271), 95–97.
Pickard, C.J., Needs, R.J., 2010. Aluminium at terapascal pressures. Nat. Mater. 9 (8), 624–627.
Ping, Y., Coppari, F., Hicks, D.G., Yaakobi, B., Fratanduono, D.E., Hamel, S., Eggert, J.H., Rygg, J.R., Smith, R.F., Swift, D.C., Braun, D.G., Boehly, T.R., Collins, G.W., 2013. Solid iron compressed up to 560 GPa. Phys. Rev. Lett. 111 (6).
Polsin, D.N., et al., 2017. Measurement of body-centered-cubic aluminum at 475 GPa. Phys. Rev. Lett. 119 (17), 175702–175704.
Porporato, A., Calabrese, S., Hueckel, T., 2019. Thermodynamic relations among isotropic material properties in conditions of plane shear stress. Entropy 21 (3), 295–309.
Qin, Z., Jung, G.S., Kang, M.J., Buehler, M.J., 2017. The mechanics and design of a lightweight three-dimensional graphene assembly. Sci. Adv. 3 (1).
Reynard, B., Price, G.D., 1990. Thermal expansion of mantle minerals at high pressures-A theoretical study. Geophys. Res. Lett. 17 (6), 689–692.
Simon, N.J., Drexler, E.S., Reed, R.P. 1992. Properties of copper and copper alloys at cryogenic temperatures. National Institutes Standards Technology, 177: 6-11, p. 7-31, 7-32.
Swenson, C.A., 1968. Equation of state of cubic solids; some generalizations. J. Phys. Chem. Solid 29 (8), 1337–1348.
Tallon, J.L., 1979. The volume dependence of elastic moduli and the Born-Durand melting hypothesis. Philos. Mag. A 39 (2), 151–161.
Tallon, J.L., 1980. The thermodynamics of elastic deformation—I. J. Phys. Chem. Solid 41 (8), 837–850.
Tallon, J.L., 1982. Crystal instability and melting. Nature 299 (5879), 188.
Tallon, J.L., Robinson, W.H., Smedley, S.I., 1977. A melting criterion based on the dilatation dependence of shear moduli. Nature 266 (5600), 337–338.
Tallon, J.L., Wolfenden, A., 1979. Temperature dependence of the elastic constants of aluminum. J. Phys. Chem. Solid 40 (11), 831–837.
Wallace, D.C., 1972. Thermodynamics of Crystals. John Wiley & Sons Inc., New York.
Wang, J., Smith, R.F., Eggert, J.H., Braun, D.G., Boehly, T.R., Reed Patterson, J., Celliers, P.M., Jeanloz, R., Collins, G.W., Duffy, T.S., 2013. Ramp compression of iron to 273 GPa. J. Appl. Phys. 114 (2), 023513.
Yehia, S., Kashwani, G., 2013. Performance of structures exposed to extreme high temperature—an overview. Open J. Civil Eng. 03 (03), 154–161.
Zha, C.-S., Boehler, R., 1985. Melting of sodium and potassium in a diamond anvil cell. Phys. Rev. B 31 (5), 3199–3201.